JOURNAL OF SPACECRAFT AND ROCKETS
Vol. 33, No. 2, March–April 1996

Vibration of Geometrically Imperfect Panels Subjected to Thermal and Mechanical Loads

L. Librescu* and W. Lin†
Virginia Polytechnic Institute and State University, Blacksburg, Virginia 24061-0219
and
M. P. Nemeth‡ and J. H. Starnes Jr.§
NASA Langley Research Center, Hampton, Virginia 23681-0001

The results of a study of the vibration response of transversely isotropic flat and curved panels subjected to temperature fields and to mechanical loads into the postbuckling load range are presented. The results were obtained using a higher-order transverse-shear-deformation theory of shallow shells that includes the effects of geometric nonlinearities and initial geometric imperfections. The results focus on the interaction between the temperature field, the applied mechanical load, and the fundamental frequency associated with small vibrations about the prebuckling and postbuckling equilibrium states. Results are presented for a wide range of temperatures and mechanical load magnitudes and of geometric parameters. The results show that transverse-shear flexibility has a significant effect on the analytical prediction of panel response and that the fundamental frequency of a panel may be substantially overestimated in the prebuckling load range and underestimated in the postbuckling load range. Results are also presented that indicate that the fundamental frequency of flat panels generally increases as the initial geometric imperfection amplitude increases for both the prebuckling and postbuckling load ranges. The results, however, also indicate that the fundamental frequency of curved panels generally decreases in the prebuckling load range and increases in the postbuckling load ranges.

Nomenclature

D	= isotropic plate bending stiffness
E, E'	= moduli of elasticity in the surface and transverse to the surface of the panel
G'	= shear modulus perpendicular to the surface of the panel
h	= panel thickness
$\tilde{L}_{11}$	= nondimensional stress resultant
ℓ_1, ℓ_2	= panel planform side lengths
m	= wave number in the x_1 direction of the panel
m_0	= mass coefficient
N_{11}	= stress resultant
n	= wave number in the x_2 direction of the panel
p_0	= nondimensional lateral pressure
$p_3(x_1, x_2)$	= lateral pressure
p_{mn}	= modal amplitudes of $p_3(x_1, x_2)$
R_2	= principal radius of curvature of a cylindrical panel
$T(x_1, x_2, x_3)$	= temperature field
T_e	= temperatures of the panel where x_3 equals $-h/2$
T_i	= temperatures of the panel where x_3 equals $h/2$
$\overset{0}{T}(x_1, x_2)$	= average temperature of the middle surface of the panel
$\overset{1}{T}(x_1, x_2)$	= temperature gradient of the panel
$\overset{0}{T}_{mn}$	= modal amplitudes of $\overset{0}{T}(x_1, x_2)$
$\overset{1}{T}_{mn}$	= modal amplitudes of $\overset{1}{T}(x_1, x_2)$
t	= time
$v_3(x_1, x_2, t)$	= displacement transverse to the panel
$\overset{0}{v}_3$	= initial geometric imperfection amplitude
$w_{mn}(t)$	= modal amplitudes
$\overset{0}{w}_{mn}$	= modal amplitudes of the initial geometric imperfection shape
$\bar{w}_{mn}$	= modal amplitudes defining a static equilibrium state
$\bar{\bar{w}}_{mn}(t)$	= modal amplitudes defining small vibrations about a static equilibrium state
$\tilde{w}_{mn}$	= eigenvector for small vibrations about a static equilibrium state
x_1, x_2	= planform coordinates of the panel
x_3	= transverse coordinate of the panel
α, α'	= coefficients of thermal expansion in the surface and transverse to the surface of the panel
$\Gamma(x_1, x_2, t)$	= Helmholtz potential function
δ_0	= nondimensional initial geometric imperfection amplitude
λ, λ'	= thermal compliances in the surface and transverse to the surface of the panel
λ_m	= nondimensional wave number in the x_1 direction of the panel
μ_n	= nondimensional wave number in the x_2 direction of the panel
ν, ν'	= Poisson's ratios in the surface and transverse to the surface of the panel
ω	= fundamental frequency of the panel
ϖ	= nondimensional fundamental frequency of the panel

Received Sept. 27, 1994; revision received Oct. 11, 1995; accepted for publication Oct. 13, 1995.

*Professor, Department of Engineering Science and Mechanics.
†Graduate Student, Department of Engineering Science and Mechanics.
‡Senior Research Engineer, Structural Mechanics Branch. Senior Member AIAA.
§Head, Structural Mechanics Branch. Fellow AIAA.

Introduction

FUTURE high-performance flight and launch vehicles, such as a supersonic transport or a hypersonic reuseable launch vehicle, have several design challenges associated with elevated temperatures caused by high speed. In 1956, Bisplinghoff[1] identified the effects of elevated temperatures on the aeroelastic behavior of high-speed aircraft structures as an especially important design consideration that needs further investigation and development. The design of other classes of high-speed vehicles are affected in a similar manner, and the same need applies for these vehicles as well. The present study addresses this need at a fundamental level by examining the

vibration of flat and curved panels subjected to thermal and mechanical loads.

Several studies of the behavior of panels and shells subjected to elevated temperatures have been conducted during the past 40 years. Recent comprehensive reviews of the behavior of plates and shells subjected to elevated temperature fields[2–4] have identified a need to understand better the effects of temperature fields on the vibration response of these structures when subjected to combined thermal and mechanical loads, especially in the postbuckling load range. Changes in the vibration characteristics of plates and shells also affect the dynamic response and flutter characteristics of these structures[5,6] that can ultimately affect the stability and control of the vehicle. With the exception of Ref. 7, it appears that previous studies of the effects of temperature or mechanical loads on the vibration characteristics of buckled structures have focused on flat plate subcomponents.[8–10] In Ref. 7, the vibration of infinitely long cylindrical panels made of isotropic material and subjected to thermal loads in the prebuckling and postbuckling equilibrium states was investigated. Other similar studies of the effects of temperature on the response of structures have focused on the dynamic behavior of heated space structures.[11]

This paper focuses on the vibration of flat and cylindrical panels made of transversely isotropic materials and subjected to combined thermal and mechanical loads in both the prebuckling and postbuckling equilibrium states. The mechanical loads include lateral pressure and in-plane compression loads, and the thermal loads include both spatially uniform and linear through-the-thickness temperature fields. The effects of initial geometric imperfections and transverse-shear deformation are included in the analysis. Results are presented that show the effects of combined mechanical and thermal loads, initial geometric imperfections, and transverse-shear deformations on the vibration response of the panels.

Analysis Description

The analysis used in the present study is based on a higher-order transverse-shear-deformation theory that includes the effects of geometric nonlinearities and initial geometric imperfections. Since the details of the theory are lengthy, only a summary of the analysis is presented in this paper. Details of the analysis can be found in Refs. 12 and 13.

Thermoelastic Constitutive Relations

The thermoelastic constitutive equations used for the present study are for homogeneous shallow shells with uniform thickness. The shell material is elastic and transversely isotropic, with the plane of isotropy coinciding with the tangent plane at each point of the shell reference surface. The corresponding constitutive equations are characterized by five elastic constants and two thermal coefficients. The elastic constants and thermal coefficients that characterize the plane of isotropy of the material are the elastic modulus E, Poisson's ratio ν, and the thermal compliance λ. The elastic modulus E', Poisson's ratio ν', the shear modulus G', and the thermal compliance λ' characterize the material behavior perpendicular to the plane of isotropy. Equations showing the relationship between the thermal compliances, λ and λ', and the corresponding coefficients of thermal expansion, α and α', are given in Refs. 14 and 15. For transversely isotropic materials, the transverse thermal expansion coefficient α' is often much larger than the tangential coefficient of thermal expansion α. In addition, the transformed reduced thermoelastic constitutive equations used in the higher-order transverse-shear-deformation theory indicate that the thermal compliances depend on the ratio of the elastic moduli E/E'. The corresponding equations based on classical shell theory do not depend on this ratio.

Nonlinear Boundary-Value Problem

In the present study, the nonlinear equations governing the dynamic response of shallow shells are posed as an extension of the classical von Kármán–Marguerre–Mushtari nonlinear shallow shell equations that include the effects of geometric imperfections and transverse-shear deformations. An Airy's stress function is used to eliminate the shell in-plane force equilibrium equations. The compatibility equation for the membrane strains is included as a primary field equation of the nonlinear boundary-value problem along with the remaining shell out-of-plane force equilibrium equation and the two moment equilibrium equations. A partially inverted form of the constitutive equations is introduced in which the membrane strains are expressed in terms of the Airy's stress function and the transverse displacement, and the bending stress resultants and transverse shear stress resultants are expressed in terms of the rotations and the transverse displacement. Substituting these special constitutive equations into the three remaining shell equilibrium equations and into the strain compatibility equation yields four coupled partial differential equations in terms of the stress function, the transverse displacement, and the two rotations. The equations are reduced further by expressing the rotations in terms of the transverse displacement $v_3(x_1, x_2, t)$ and a potential function $\Gamma(x_1, x_2, t)$, where x_1 and x_2 are the planform coordinates of a panel an t denotes time. Substituting the resulting expression into the out-of-plane force equilibrium equation yields an equation in terms of the stress function and the transverse displacement, whereas its substitution into the moment equilibrium equations yields a single Helmholtz type boundary-layer equation in Γ that is totally uncoupled from the other equations. In general, however, the boundary-value problem remains coupled through the five boundary conditions at each edge of the shell.

The boundary conditions considered in the present study are simply supported boundary conditions. For these boundary conditions, the edges of a shell are free to move tangentially when unloaded. For simply supported boundary conditions, the nonlinear boundary-value problem is uncoupled with respect to the potential function Γ and the solution to the Helmholtz type boundary-layer equation in Γ is $\Gamma = 0$. Thus, for shells with simply supported edges, the nonlinear boundary-value problem reduces to two partial differential equations in terms of the Airy's stress function and the transverse deflection v_3. These two equations are referred to herein as the von Kármán type compatibility and transverse force equilibrium equations.

Solution of the Nonlinear Equations

The nonlinear boundary-value problem in the present study is solved using Galerkin's method. First, the transverse deflection is expressed in terms of functions that satisfy the simply supported boundary conditions

$$v_3(x_1, x_2, t) = w_{mn}(t) \sin \lambda_m x_1 \sin \mu_n x_2 \tag{1}$$

where $\lambda_m = m\pi/\ell_1$, $\mu_n = n\pi/\ell_2$, and $w_{mn}(t)$ are the modal amplitudes, and ℓ_1 and ℓ_2 are the panel planform side lengths. Following the results presented in Ref. 16, the initial geometric imperfection $\overset{0}{v}_3$ is expressed as

$$\overset{0}{v}_3(x_1, x_2) = \overset{0}{w}_{mn} \sin \lambda_m x_1 \sin \mu_n x_2 \tag{2}$$

where $\overset{0}{w}_{mn}$ are the modal amplitudes of the initial geometric imperfection shape. Similarly, the applied temperature and pressure fields are represented by

$$\overset{0}{T}(x_1, x_2) = \sum_{m=1}^{M} \sum_{n=1}^{N} \overset{0}{T}_{mn} \sin \lambda_m x_1 \sin \mu_n x_2 \tag{3}$$

$$\overset{1}{T}(x_1, x_2) = \sum_{m=1}^{M} \sum_{n=1}^{N} \overset{1}{T}_{mn} \sin \lambda_m x_1 \sin \mu_n x_2 \tag{4}$$

$$p_3(x_1, x_2) = \sum_{m=1}^{M} \sum_{n=1}^{N} p_{mn} \sin \lambda_m x_1 \sin \mu_n x_2 \tag{5}$$

where $\overset{0}{T}$ and $\overset{1}{T}$ enter into the analysis through the constitutive equations and are expressed in terms of the temperatures of the panel with the transverse coordinates $x_3 = h/2$ and $-h/2$, which are denoted by T_i and T_e, respectively, and are given by

$$\overset{0}{T} = \frac{T_i + T_e}{2} \tag{6}$$

$$\overset{1}{T} = \frac{T_i - T_e}{h} \tag{7}$$

The temperature field is given by

$$T(x_1, x_2, x_3) = \overset{0}{T}(x_1, x_2) + x_3 \overset{1}{T}(x_1, x_2) \tag{8}$$

The displacement expansions are substituted into the von Kármán type compatibility equation, and the Airy's stress function is obtained by solving the resulting linear nonhomogeneous partial differential equation. The remaining nonlinear partial differential equation is the von Kármán type equilibrium equation and is converted into a set of nonlinear ordinary differential equations using Galerkin's method. This procedure yields the following set of $M \times N$ nonlinear ordinary differential equations for each set of wave forms determined by the index pair (m, n):

$$A_{rs}\ddot{w}_{rs} + R_{rs}w_{rs} + p_{rs}B_{rs} - \overset{1}{T}_{rs}C_{rs} + P_1\left[w_{rs}, \overset{0}{w}_{rs}, \tilde{L}_1, \tilde{L}_2\right] + P_2\left[w_{rs}^2, \overset{0}{w}_{rs}\right] + P_3\left[w_{rs}^3, \overset{0}{w}_{rs}\right] + P_4\left[w_{rs}, \overset{0}{w}_{rs}, \overset{0}{T}_{rs}, \overset{1}{T}_{rs}\right] = 0 \tag{9}$$

where the indices r and s are not summed and have the values $r = 1, 2, \ldots, M$ and $s = 1, 2, \ldots, N$. In Eq. (9), P_1 and P_4, P_2, and P_3 are linear, quadratic, and cubic polynomials of the unknown modal amplitudes $w_{rs}(t)$, respectively. The coefficients A_{rs}, B_{rs}, C_{rs}, and R_{rs} are constants that depend on the material and geometric properties of the shell and $\tilde{L}_1$ and $\tilde{L}_2$ are normalized forms of the inplane stress resultants representing the mechanical loads.

Equations for Static-Equilibrium States and Small Vibrations

The main emphasis of the present study is on the vibration response of flat and cylindrical panels that are loaded quasistatically into the postbuckling load range. To obtain the equations that govern the static prebuckling and postbuckling equilibrium states and small vibrations about these equilibrium states, the unknown modal amplitudes are expressed as

$$w_{rs}(t) = \bar{w}_{rs} + \bar{\bar{w}}_{rs}(t) \tag{10}$$

where $\bar{\bar{w}}_{rs}(t)$ represents small vibrations about a mean static equilibrium configuration described by $\bar{w}_{rs}$. The vibrations are considered small compared to $\bar{w}_{rs}$ and the imperfection amplitude $\overset{0}{w}_{rs}$ in the sense that

$$[\bar{\bar{w}}_{rs}(t)]^2 \ll \bar{w}_{rs}, \overset{0}{w}_{rs} \tag{11}$$

for all values of the indices r and s. The equations for the static prebuckling and postbuckling equilibrium states are obtained by discarding the inertia terms given by $A_{rs}\ddot{w}_{rs}$ in Eq. (9) and recognizing that the solution to the resulting equation is $\bar{w}_{rs}$. The equations for small vibrations about a given static equilibrium state are then obtained by substituting Eq. (10) into Eq. (9) and enforcing the smallness condition given by Eq. (11). The resulting equations of motion are given by

$$A_{rs}\ddot{\bar{\bar{w}}}_{rs}(t) + G_{rs}\bar{\bar{w}}_{rs}(t) = 0 \tag{12}$$

where

$$G_{rs} = G_{rs}\left(\bar{w}_{rs}, \bar{w}_{rs}^2, \bar{w}_{rs}^3, \overset{0}{w}_{rs}, p_{rs}, \overset{0}{T}_{rs}, \overset{1}{T}_{rs}\right) \tag{13}$$

for values of $r = 1, 2, \ldots, M$ and $s = 1, 2, \ldots, N$. The constant coefficients A_{rs} are functions of the material and geometric properties of the shell.

Equation (12) govern small vibrations about a given equilibrium state and are solved for synchronous motion by expressing $\bar{\bar{w}}_{rs}(t)$ as

$$\bar{\bar{w}}_{rs}(t) = \tilde{w}_{rs}e^{i\omega_{rs}t} \tag{14}$$

Substituting Eq. (14) into Eq. (12) yields an algebraic eigenvalue problem given by

$$G_{rs}\tilde{w}_{rs} = \omega_{rs}^2 A_{rs}\tilde{w}_{rs} \tag{15}$$

for values of $r = 1, 2, \ldots, M$ and $s = 1, 2, \ldots, N$. The frequencies ω_{rs} in Eq. (15) are the unknown quantities to be found and the corresponding amplitudes $\tilde{w}_{rs}$ are indeterminate.

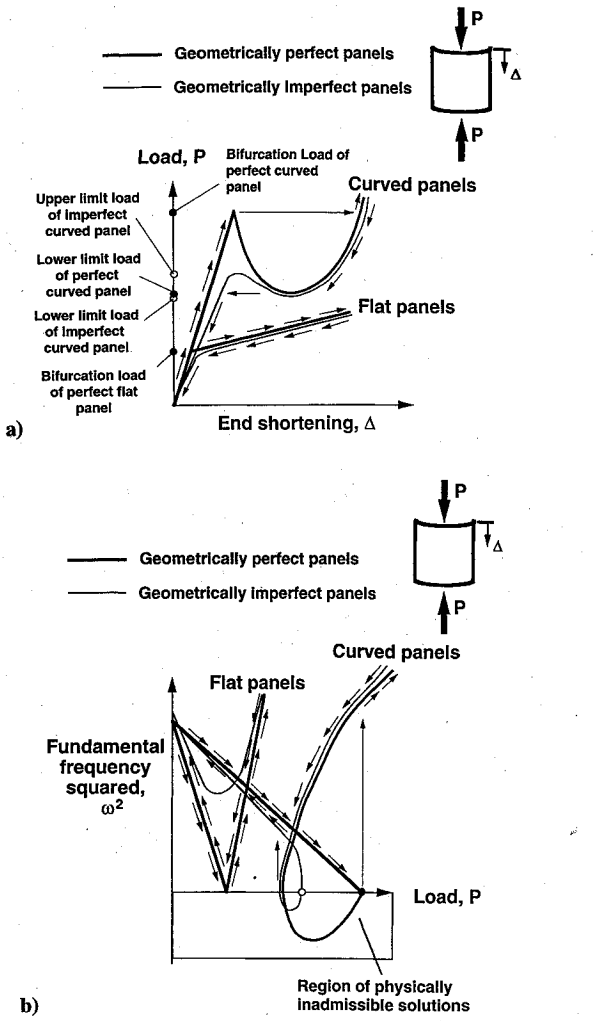

Fig. 1 Response curves for flat and curved panels loaded in compression: a) static load vs end-shortening curves and b) load frequency curves.

Computational Approach

The solution of Eq. (12) begins with the determination of the static equilibrium states of a flat or curved panel over a given range of a load parameter. The static load vs end-shortening curves for these structures with and without initial geometric imperfections are shown in Fig. 1a. The curves in this figure indicate that the load vs end-shortening curves for flat and curved panels are significantly different. Flat panels exhibit a stable postbuckling response for which no reduction in load-carrying capacity occurs at buckling, and the response is not sensitive to initial geometric imperfections. This characteristic of flat panels is indicated in the figure by the close proximity of the curves for the corresponding imperfect and perfect flat panels and the positive slopes of the curves for values of the load greater than the bifurcation load.

Curved panels, however, exhibit an unstable postbuckling response and the load-carrying capacity of the curved panel is reduced to a value below the bifurcation load when the response jumps to a new stable equilibrium configuration at a limit point. The response of curved panels can be very sensitive to initial geometric imperfections. This characteristic of curved panels is indicated in Fig. 1a by the lack of close proximity of the bifurcation load of a perfect curved panel and the limit point of the corresponding imperfect curved panel and by the negative slope of the load vs end-shortening curve of the perfect curved panel in the initial postbuckling load range.

The static equilibrium configuration for a given flat or curved panel is obtained by solving the nonlinear algebraic equations given by Eqs. (9) via Newton's method. After obtaining the static equilibrium configuration of a panel for given values of the loading parameters, the coefficients A_{rs} and G_{rs} in Eq. (12) are computed, and the

linear algebraic eigenvalue problem defined by Eq. (15) is solved. In some instances, Eq. (15) possesses negative eigenvalues that correspond to pure imaginary fundamental vibration frequencies. For the panels investigated herein, the pure imaginary fundamental frequencies correspond to unstable branches of the postbuckling equilibrium path as depicted in Fig. 1b.

Results and Discussion

The results presented in the present paper are for small vibrations about the static prebuckling and postbuckling equilibrium states of simply supported flat and curved panels. The panels considered have a square planform with dimensions $\ell_1 = \ell_2 = \ell$ and consist of a single elastic layer of transversely isotropic material. For all of the results presented herein, the elastic moduli and coefficients of thermal expansion are constant nondimensional ratios with values of $E'/E = 5$ and $\alpha'/\alpha = 15$, respectively. The elastic-modulus-to-shear-modulus ratio E/G' is varied to determine the effects of transverse-shear flexibility on the results. The results are presented in the form of interaction curves that relate the applied load to the square of the fundamental frequency as a function of the temperature field, geometric imperfection amplitude, and degree of transverse-shear flexibility. The square of the fundamental frequency ω^2, the applied inplane compression load N_{11}, and the applied transverse pressure load p_3 are represented in the figures by the following nondimensional parameters:

$$\varpi^2 = \frac{\omega^2 m_0 \ell^4}{\pi^4 D} \tag{16}$$

$$\tilde{L}_{11} = \frac{N_{11}\ell^2}{\pi^4 D} \tag{17}$$

$$p_0 = p\ell^4/Dh \tag{18}$$

where m_0 is an inertia coefficient, D is given by

$$D = \frac{Eh^3}{12(1-\nu^2)} \tag{19}$$

and $p = p_3(\ell/2, \ell/2)$. At buckling, the parameter $\tilde{L}_{11}$ corresponds to the well-known definition of the buckling coefficient for isotropic panels. Similarly, a nondimensional initial geometric imperfection amplitude δ_0 is used in the figures and is given by

$$\delta_0 = \frac{\mathring{v}_3(\ell/2, \ell/2)}{h} \tag{20}$$

Several results are presented that indicate the importance of transverse-shear flexibility. The degree of transverse-shear flexibility is indicated in the figures by the ratio E/G'. A value of $E/G' = 30$, corresponding to panels with a moderate degree of transverse-shear flexibility, and a value of panel length-to-thickness $\ell/h = 20$, corresponding to moderately thick panels, were used to obtain the results unless otherwise noted in the figures. For all of the results presented, the temperature field is specified to be a single half-sine wave along each coordinate direction and on both bounding surfaces of the panels considered. For this temperature distribution, T_i and T_e represent the amplitudes of the temperature distributions on the bounding surfaces of a panel. Two through-the-thickness temperature distributions are considered in the present study. One temperature distribution has the same temperature ($T_i = T_e$) on both panel surfaces, and the other temperature distribution has unequal temperatures ($T_i \neq T_e$) on the panel surfaces. For all results presented involving a through-the-thickness temperature gradient, a constant amplitude value of $T_e = 70°F$ (21°C) is used. Results for flat panels are presented in Figs. 2–6, and results for cylindrical curved panels are presented in Figs. 7–11.

Results for Flat Panels

The effects of uniaxial compressive edge loads on the fundamental vibration frequency of geometrically perfect panels are shown in Fig. 2 for two uniform temperature distributions of amplitude given by $T_i = T_e = 70°F$ (21°C) and $T_i = T_e = 1500°F$ (815°C). The

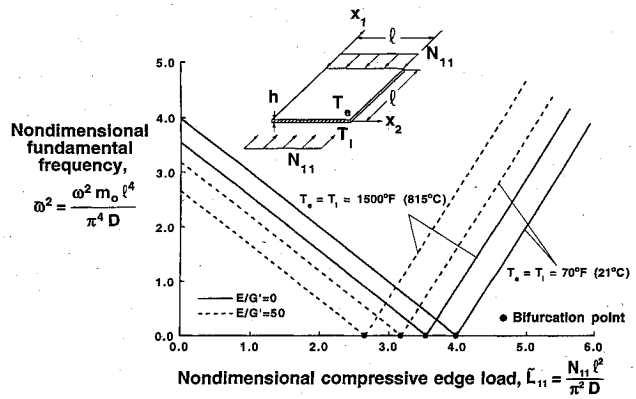

Fig. 2 Effects of transverse-shear flexibility and uniform temperature distribution on the fundamental frequency of flat compression-loaded square panels.

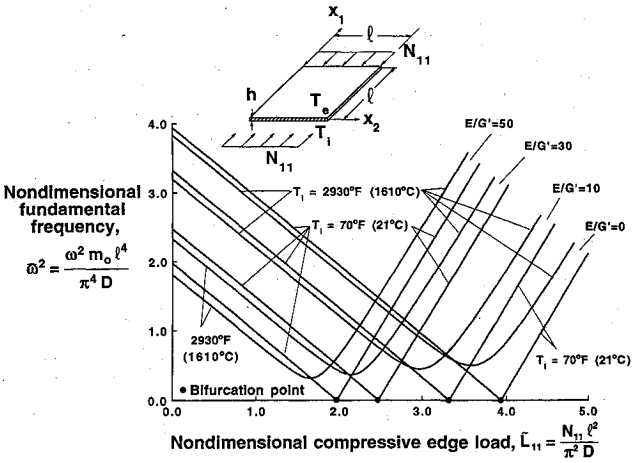

Fig. 3 Effects of transverse-shear flexibility and through-the-thickness temperature gradient on the fundamental frequency of flat compression-loaded square panels; $\ell/h = 10$, $T_e = 70°F$ (21°C).

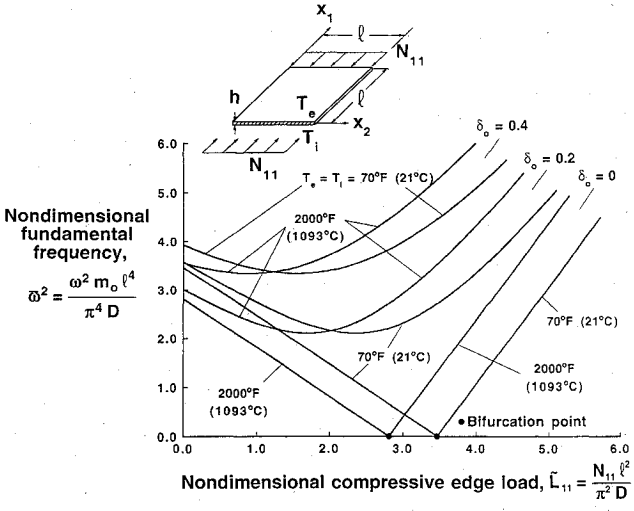

Fig. 4 Effects of uniform temperature distribution and initial imperfection amplitude δ_0 on the fundamental frequency of flat compression-loaded square panels; $E/G' = 30$.

solid lines in the figure correspond to results for panels with negligible transverse-shear flexibility ($E/G' = 0$). The dashed lines in the figure correspond to results for panels with a high degree of transverse-shear flexibility ($E/G' = 50$). The results indicate that the fundamental frequency decreases linearly with increasing edge load prior to buckling for a given prebuckling thermal load. Increasing the prebuckling load increases the in-plane compression load in the panel that reduces the fundamental frequency resulting from the additional bending moment caused by the nonlinear coupling of the

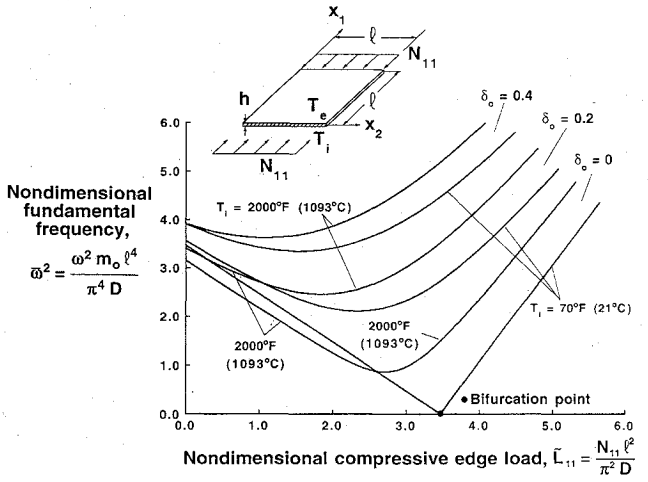

Fig. 5 Effects of through-the-thickness temperature gradient and initial imperfection amplitude δ_0 on the fundamental frequency of flat compression-loaded square panels; $E/G' = 30$, $T_e = 70°F$ (21°C).

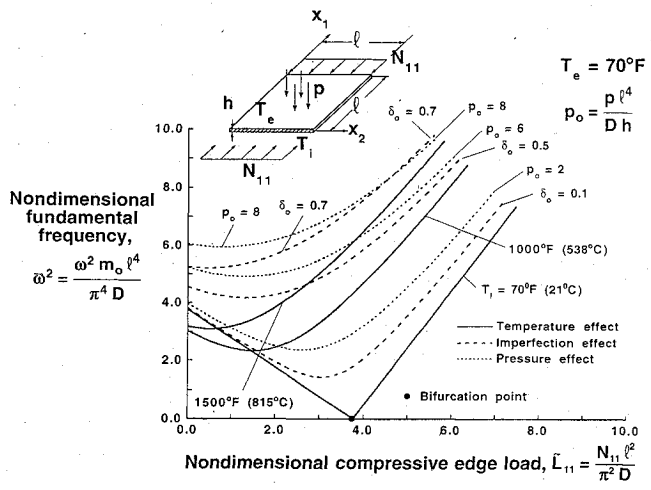

Fig. 6 Effects of temperature distribution, initial imperfection amplitude δ_0, and lateral pressure on the fundamental frequency of flat compression-loaded square panels; $E/G' = 30$, $T_e = 70°F$ (21°C), $\ell/h = 40$.

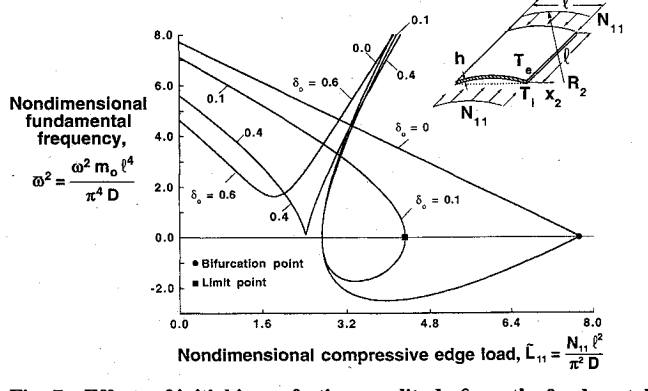

Fig. 7 Effects of initial imperfection amplitude δ_0 on the fundametal frequency of compression-loaded cylindrical panels with square planform; $\ell/R_2 = 0.5$, $E/G' = 30$, $T_i = T_e = 70°F$ (21°C).

inplane load with the out-of-plane displacements. The fundamental frequency decreases as either the transverse-shear flexibility or the temperature increases in the prebuckling loading range. At buckling, the fundamental frequency is zero valued, as indicated by the filled circles in the figure. The highest value of the buckling coefficient, $\tilde{L}_{11} = 4$, is predicted for the panels with negligible transverse-shear flexibility and $T_i = T_e = 70°F$ (21°C). The results also indicate that the buckling coefficient decreases as the temperature or the degree of transverse-shear flexibility increases. The results indicate that

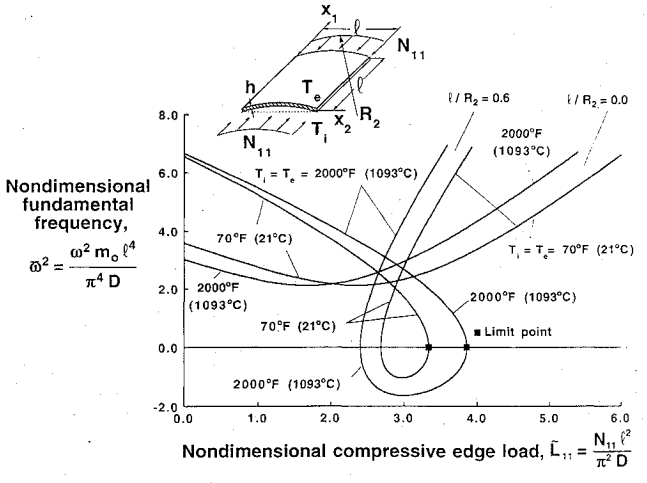

Fig. 8 Effects of panel curvature and uniform temperature distribution on the fundamental frequency of imperfect compression-loaded cylindrical panels with square planform; $E/G' = 30$, $\delta_0 = 0.2$.

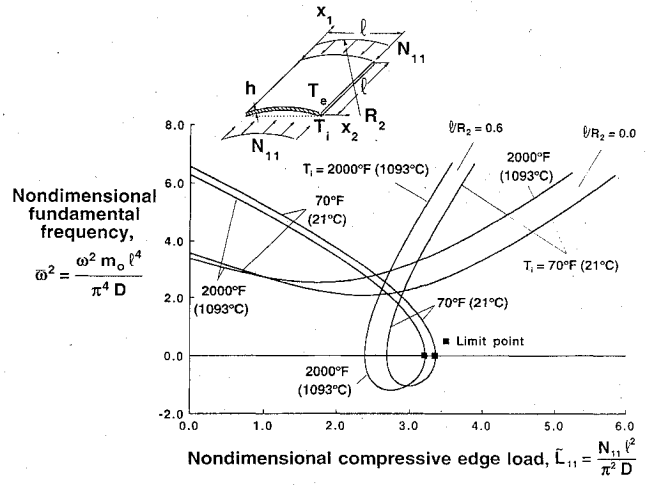

Fig. 9 Effects of panel curvature and through-the-thickness temperature gradient on the fundamental frequency of imperfect compression-loaded cylindrical panels with square planform; $E/G' = 30$, $\delta_0 = 0.2$, $T_e = 70°F$ (21°C).

the fundamental frequency increases as the load increases above the buckling load. Panels with negligible transverse-shear flexibility or a lower temperature have lower fundamental frequencies for a given load level. The increase in fundamental frequency above the buckling load is attributed to the redistribution of internal load and the change in panel geometry that occurs after buckling. When a flat panel buckles, it deforms into a mode shape that is a curved surface. The curvature of the buckled panel increases the overall panel bending stiffness that increases the fundamental frequency.

The effects of a through-the-thickness temperature gradient and transverse-shear flexibility on the interaction of an applied compression load and the fundamental frequency of thin panels ($\ell/h = 10$) are shown in Fig. 3. The through-the-thickness temperature gradient corresponds to surface temperature amplitudes $T_e = 70°F$ (21°C) and $T_i = 2930°F$ (1610°C). Results corresponding to a uniform temperature distribution with $T_i = T_e = 70°F$ (21°C) are also shown in the figure for comparison. The panels with uniform temperature distributions have perfectly flat prebuckling shapes and buckle at the bifurcation points indicated by the filled circles on the abscissa. The panels with a through-the-thickness temperature gradient have small out-of-plane deflections at the onset of loading and, as a result, the curves corresponding to $T_i = 2930°F$ (1610°C) in the figure do not have bifurcation points. Results for panels with a wide range of transverse-shear flexibility given by $E/G' = 0$, 10, 30, and 50 are shown in the figure. The results for the through-the-thickness temperature gradient indicate a similar interaction between an applied compression load and the fundamental frequency of the panels as

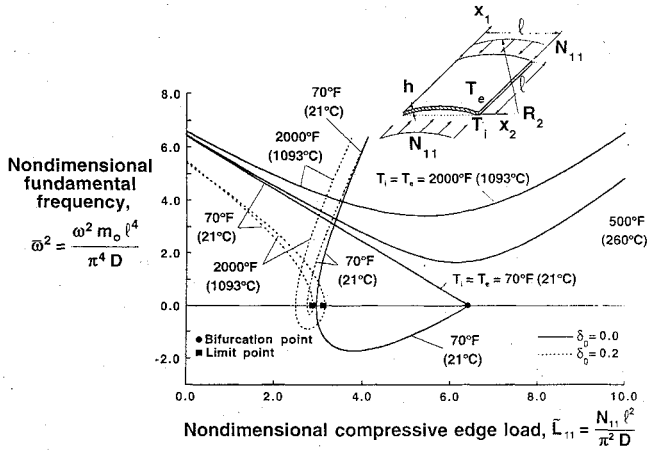

Fig. 10 Effects of uniform temperature distribution and initial imperfection amplitude δ_0 on the fundamental frequency of compression-loaded cylindrical panels with square planform; $\ell/R_2 = 0.5$, $E/G' = 30$, $\ell/h = 20$.

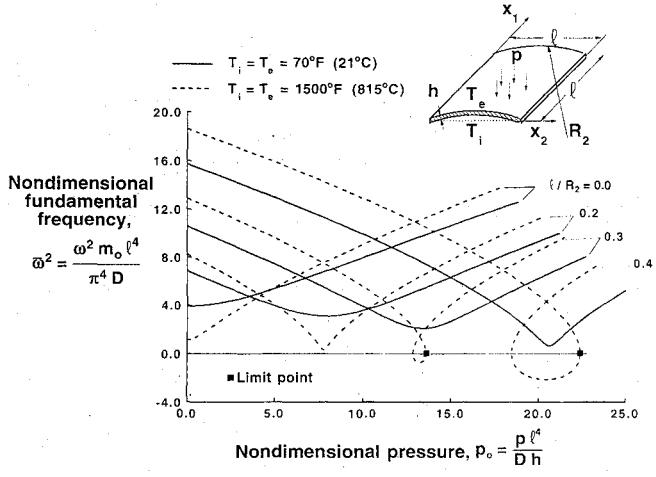

Fig. 11 Effects of panel curvature and uniform temperature distribution on the fundametal frequency of cylindrical panels with square planform and loaded by lateral pressure; $E/G' = 50$.

indicated for panels subjected to a uniform temperature gradient. The fundamental frequency decreases monotonically as the prebuckling load increases and then increases monotonically as the postbuckling load increases. The results indicate that increasing the transverse-shear flexibility E/G' decreases the prebuckling fundamental frequency and increases the postbuckling fundamental frequency for a given applied load level. The results also indicate that the fundamental frequency decreases in the prebuckling load range and increases in the postbuckling load range as the magnitude of the through-the-thickness temperature gradient increases. The results indicate that transverse-shear flexibility can significantly influence the response of a panel in both the prebuckling and postbuckling load ranges and should not be neglected in the analysis and design of panels with this type of loading conditions.

The effects of initial geometric imperfections and a uniform temperature distribution on the interaction of an applied compression load and the fundamental frequency of panels with moderate transverse-shear flexibility ($E/G' = 30$) are shown in Fig. 4. Results are given for surface temperature amplitudes $T_i = T_e = 70°F$ (21°C) and 2000°F (1093°C) and for three different imperfection amplitudes given by $\delta_0 = 0$, 0.2, and 0.4, where δ_0 equals the magnitude of the imperfection amplitude at the panel center divided by the panel thickness, and the imperfection shape is a half-sine wave along each coordinate direction. The results shown in the figure for $\delta_0 = 0$ reveal the occurrence of buckling bifurcation indicated by the filled circles on the abscissa consistent with the behavior of flat panels without imperfections. The results indicate that the fundamental frequencies increase as the imperfection amplitude increases for both the prebuckling and postbuckling load ranges and for both temperature distributions. The panels with $T_i = T_e = 70°F$ (21°C) generally have higher fundamental frequencies in the prebuckling load range than the panels with $T_i = T_e = 2000°F$ (1093°C). The opposite effect is predicted in the postbuckling load range.

The effects of a through-the-thickness temperature gradient and an initial imperfection on the interaction of an applied compression load and the fundamental frequency of panels with moderate transverse-shear flexibility ($E/G' = 30$) are shown in Fig. 5. The through-the-thickness temperature gradient corresponds to surface temperatures of amplitudes $T_e = 70°F$ (21°C) and $T_i = 2000°F$ (1093°C). Results corresponding to a uniform temperature distribution with $T_i = T_e = 70°F$ (21°C) are also shown in the figure for comparison. The results shown in the figure for $\delta_0 = 0$ and $T_i = T_e = 70°F$ (21°C) have bifurcation points indicated by the filled circles on the abscissa consistent with the behavior of flat panels without imperfections. The results indicate that the fundamental frequencies increase as the imperfection amplitude increases for both the prebuckling and postbuckling load ranges and with or without a temperature gradient. Panels with a temperature gradient have higher fundamental frequencies than corresponding panels without a temperature gradient for most values of the applied load when the imperfection amplitude is nonzero.

The effects of a through-the-thickness temperature gradient, a transverse pressure load of amplitude p_0, and an initial geometric imperfection amplitude δ_0 on the interaction of applied compression loads and the fundamental frequency of thick panels ($\ell/h = 40$) with $E/G' = 30$ are shown in Fig. 6. Results for a uniform temperature distribution [$T_i = T_e = 70°F$ (21°C)], $\delta_0 = 0$, and $p_0 = 0$ are shown in the figure for comparison, and these results have a bifurcation point indicated by the filled circle on the abscissa consistent with the behavior of a perfectly flat panel. The solid lines on the figure are the results for the through-the-thickness temperature gradient, the long dashed lines are the results for the transverse pressure load, and the short dashed lines are the results for the initial geometric imperfections. The results indicate that a through-the-thickness temperature gradient, a transverse pressure load, and an initial geometric imperfection affect the panel behavior in a similar manner. A through-the-thickness temperature gradient, a transverse pressure load, or an initial imperfection cause out-of-plane prebuckling deformation from the onset of loading, which causes the similar behavior.

Results for Curved Panels

Initial geometric imperfections have a strong influence on the design of compression-loaded curved panels. The effects of initial geometric imperfections on the interaction of applied compression loads and the fundamental frequency of curved panels with moderate transverse-shear flexibility ($E/G' = 30$) are shown in Fig. 7. Results are given for a curved panel with a length-to-radius ratio $\ell/R_2 = 0.5$, a uniform temperature distribution with $T_i = T_e = 70°F$ (21°C) and for four initial imperfection amplitudes given by $\delta_0 = 0$, 0.1, 0.4, and 0.6. The bifurcation point for the geometrically perfect curved panel is indicated on the abscissa by the filled circle, and the collapse or limit point for a geometrically imperfect curved panel is indicated by the filled square. In general, the results indicate that the fundamental frequency decreases monotonically with increasing prebuckling load and increases monotonically in the postbuckling load range. More specifically, the fundamental frequency of the curved panels with $\delta_0 = 0$ and 0.1 decrease monotonically with increasing prebuckling load. At buckling or collapse, a curved panel changes equilibrium configuration and follows an unstable equilibrium path corresponding to pure imaginary values of the fundamental frequency. Once back on the stable postbuckling path (indicated by real values of the fundamental frequency), the fundamental frequency increases monotonically with increasing load. A limit point is not present for the panels with the larger imperfection amplitudes given by $\delta_0 = 0.4$ and 0.6. For these cases, the panel response includes large nonlinear deformations as the applied load increases, and the results correspond to the monotonically increasing load-shortening results for flat panels with large initial imperfections. The load-frequency results for these curved panels

are similar to the results for flat panels with large initial geometric imperfection amplitudes.

The effects of panel curvature and uniform temperature distributions on the interaction of applied compression loads and the fundamental frequency of imperfect curved panels with $E/G' = 30$ and $\delta_0 = 0.2$ are shown in Fig. 8. Results are presented for surface temperature amplitudes $T_i = T_e = 70°F$ (21°C) and 2000°F (1093°C) and for a length-to-radius ratio $\ell/R_2 = 0.6$. Results for a flat panel with $\ell/R_2 = 0$ are shown for comparison. The results indicate that curved panels generally have higher fundamental frequencies in both the prebuckling and postbuckling load ranges than flat panels. The curved panels with $T_i = T_e = 2000°F$ (1093°C) have higher fundamental frequencies over the entire load range than the curved panels with the lower temperature. These results are different from the results for the flat panels. The flat panels with $T_i = T_e = 70°F$ (21°C) generally have the higher fundamental frequencies in the prebuckling load range, and the flat panels with $T_i = T_e = 2000°F$ (1093°C) have the higher frequencies in the postbuckling load range.

The effects of panel curvature and a through-the-thickness temperature gradient on the interaction of an applied compression load and the fundamental frequency of imperfect curved panels with $E/G' = 30$ and $\delta_0 = 0.2$ are shown in Fig. 9. Results for a flat panel with a uniform temperature distribution with $T_i = T_e = 70°F$ (21°C) are included for comparison. The results indicate that the fundamental frequency of the curved panels decreases monotonically with increasing prebuckling load and increases monotonically in the stable postbuckling load range. The results also indicate that a through-the-thickness temperature gradient generally decreases the fundamental frequency of both the flat and curved panels in the prebuckling load range and increases the frequency in the postbuckling load range.

The effects of initial imperfection amplitude and a uniform temperature distribution on the interaction of an applied compression load and the fundamental frequency for curved panels with a moderate degree of transverse-shear flexibility ($E/G' = 30$) and $\ell/R_2 = 0.5$ are shown in Fig. 10. Results for surface temperatures of amplitude $T_i = T_e = 70°F$ (21°C), 500°F (260°C), and 2000°F (1093°C) are shown in the figure for geometrically perfect panels. The solid and dashed lines in the figure correspond to results for $\delta_0 = 0$ and 0.2, respectively. These results indicate that an initial imperfection can significantly affect the behavior of curved panels with uniform temperature distributions.

The effects of curvature and a uniform temperature distribution on the response of curved panels loaded with external lateral pressure are shown in Fig. 11. These results correspond to thick ($\ell/h = 50$) geometrically perfect panels with a high degree of transverse-shear flexibility ($E/G' = 50$). The solid and dashed lines in the figure correspond to results for $T_i = T_e = 70°F$ (21°C) and 1500°F (815°C), respectively. These results indicate that increasing the panel curvature for this type of loading increases the fundamental frequency in the prebuckling range and decreases the frequency in the postbuckling load range. The results also indicate that increasing the temperature generally increases the fundamental frequency of the panels. The results indicate that the fundamental frequency decreases monotonically as the prebuckling load increases followed by a monotonic increase in the frequency in the postbuckling load range.

Concluding Remarks

The results of a parametric study of the vibration response of flat and curved panels subjected to thermal and mechanical loads are presented. The mechanical loads considered in the study are uniform uniaxial compressive edge loads and transverse lateral pressure. The temperature fields considered are associated with spatially uniform heating over the panel surfaces and a linear through-the-thickness temperature gradient. The analytical model used in the study is based on a higher-order transverse-shear-deformation theory of shallow shells that incorporates the effects of geometric nonlinearites and initial geometric imperfections. Results are presented for simply supported panels made from a single layer of transversely isotropic material. The results identify the interactions of applied compression loads and the fundamental frequencies of the panels in both the prebuckling and postbuckling equilibrium states. The results show that transverse-shear flexibility, initial geometric imperfections, temperature gradients, and transverse lateral pressure affect the interaction of an applied compression load and the fundamental frequency of both flat and curved panels. In general, the fundamental frequency decreases monotonically as the applied compression load increases in the prebuckling load range, but increases monotonically as the applied compression load increases in the postbuckling load range.

Acknowledgment

The work reported herein was partially supported by NASA Grant NAG1-1300.

References

[1]Bisplinghoff, R. L., "Some Structural and Aeroelastic Considerations of High-Speed Flight" (The Nineteenth Wright Brothers Lecture), *Journal of the Aeronautical Sciences*, Vol. 23, No. 4, 1956, pp. 289–321.

[2]Ziegler, F., and Rammerstorfer, F. G., "Thermoelastic Stability," *Thermal Stresses III*, edited by R. B. Hetnarsky, North-Holland, Amsterdam, 1989, Chap. 2, pp. 107–189.

[3]Tauchert, T. R., "Thermally Induced Flexure, Buckling and Vibration of Plates," *Applied Mechanics Reviews*, Vol. 44, No. 8, 1991, pp. 347–360.

[4]Noor, A. K., and Burton, W. S., "Computational Models for High-Temperature Multilayered Composite Plates and Shells," *Applied Mechanics Reviews*, Vol. 45, No. 10, 1992, pp. 414–446.

[5]Liaw, D. G., "Supersonic Flutter of Laminated Thin Plates with Thermal Effects," *Journal of Aircraft*, Vol. 30, No. 1, 1993, pp. 105–111.

[6]Abbas, J. F., Ibrahim, R. A., and Gibson, R. I., "Nonlinear Flutter of Orthotropic Composite Panels Under Aerodynamic Heating," *AIAA Journal*, Vol. 31, No. 8, 1993, pp. 1478–1488.

[7]Kornecki, A., "On the Thermal Buckling and Free Vibration of Cylindrical Panels Heated from Inside," *Bulletin of the Research Council of Israel*, Vol. 11C, No. 1, 1962, pp. 123–140.

[8]Bisplinghoff, R. L., and Pian, T. H. H., "On the Vibrations of Thermally Buckled Bars and Plates," *Proceedings of the 9th International Congress for Applied Mechanics*, Brussels, Belgium, Vol. 7, 1957, pp. 307–318.

[9]Yang, T. Y., and Han, A. D., "Buckled Plate Vibrations and Large Amplitude Vibrations Using High-Order Triangular Elements," *AIAA Journal*, Vol. 21, No. 5, 1983, pp. 758–766.

[10]Zhou, R. C., Xue, D. Y., Mei, C., and Gray, C. C., "Vibration of Thermally Buckled Composite Plates with Initial Deflections Using Triangular Elements," AIAA Paper 93-1321, April 1993.

[11]Thorton, E. A., and Foster, R. S., "Dynamic Response of Rapidly Heated Space Structures," *Computational Nonlinear Mechanics in Aerospace Engineering*, edited by S. N. Atluri, Vol. 146, Progress in Astronautics and Aeronautics, AIAA, Washington, DC, 1991, pp. 451–477.

[12]Librescu, L., and Chang, M.-Y., "Effects of Geometric Imperfections on Vibration of Compressed Shear Deformable Laminated Composite Curved Panels," *Acta Mechanica*, Vol. 96, 1993, pp. 203–224.

[13]Librescu, L., and Chang, M.-Y., "Vibration of Compressively Loaded Shear Deformable Flat Panels Exhibiting Initial Geometric Imperfections," *AIAA Journal*, Vol. 30, No. 11, 1992, pp. 2793–2795.

[14]Terner, E., "On Thermal Stresses in Certain Transversely Isotropic, Pyrolitic Materials," *Proceedings of the 4th U.S. National Congress of Applied Mechanics*, American Society of Mechanical Engineers, New York, 1962, pp. 1147–1152.

[15]Librescu, L., *Elasto-Statics and Kinetics of Anisotropic and Heterogeneous Shell-Type Structures*, Noordhoff International, Leyden, The Netherlands, 1975, Chap. 3.

[16]Seide, P., "A Reexamination of Koiter's Theory of Initial Postbuckling Behavior and Imperfection Sensitivity of Structures," *Thin Shell Structures: Theory, Experiment and Design*, edited by Y. C. Fung and E. E. Sechler, Prentice–Hall, Englewood Cliffs, NJ, 1974, pp. 59–80.

E. A Thornton
Associate Editor